Макрогетероциклы
http://macroheterocycles.isuct.ru

DOI: 10.6060/mhc210439s

Amphiphilic *N*–Oligoethyleneglycol–imidazolium Derivatives of *p*–*tert*–Butylthiacalix[4]arene: Synthesis, Aggregation and Interaction with DNA

B. Kh. Gafiatullin,[a] D. D. Radaev,[a] M. V. Osipova,[a] E. D. Sultanova,[a@] V. A. Burilov,[a] S. E. Solovieva,[b] and I. S. Antipin[a]

[a]*Kazan Federal University, 420008 Kazan, Russian Federation*
[b]*Arbuzov Institute of Organic and Physical Chemistry, FRC Kazan Scientific Center, Russian Academy of Sciences, 420088 Kazan, Russian Federation*
[@]*Corresponding author e-mail: elsultanova123@gmail.com*

New water-soluble derivatives of p-tert-butylthiacalix[4]arene have been synthesized in the stereoisomeric form 1,3-alternate with butyl and tetradecyl groups on one side of the macrocyclic platform and tri/tetraethylene glycol substituents on the other. The aggregation characteristics of macrocycles in the aquatic environment (CAC, aggregate size, zeta potential) have been studied. It has been demonstrated that the resulting aggregates have the ability to solubilize the lipophilic azo dye Orange OT, and the solubilizing ability significantly increases on going from butyl to tetradecyl derivatives. Using the methods of dynamic and electrophoretic light scattering and fluorimetry with ethidium bromide as a probe, it was shown that the obtained macrocycles interact with the DNA of the calf thymus. It was found that the efficiency of the interaction is greatly influenced by the length of the oxyethyl fragments: macrocycles containing tetraethylene glycol fragments are more effective than triethylene glycol analogs, causing a 2-fold compaction of DNA.

Keywords: Thiacalix[4]arene, imidazole, amphiphiles, calf thymus DNA, ethidium bromide, solubilizing capacity.

Амфифильные *N*–олигоэтиленгликоль–имидазолиевые производные *n*–*трет*–бутилтиакаликс[4]арена: синтез, агрегация и взаимодействие с ДНК

Б. Х. Гафиатуллин,[a] Д. Д. Радаев,[a] М. В. Осипова,[a] Э. Д. Султанова,[a@] В. А. Бурилов,[a] С. Е. Соловьева,[b] И. С. Антипин[a]

[a]*Казанский (Приволжский) федеральный университет, 420008 Казань, Республика Татарстан, Россия*
[b]*Институт органической и физической химии им. А.Е. Арбузова ФИЦ Казанский научный центр РАН, 420088 Казань, Республика Татарстан, Россия*
[@]*E-mail: elsultanova123@gmail.com*

Синтезированы новые водорастворимые производные п-трет-бутилтиакаликс[4]арена в стереоизомерной форме 1,3-альтернат с бутильными и тетрадецильными группами с одной стороны макроциклической платформы и три/тетраэтиленгликолевыми заместителями – с другой. Исследованы агрегационные характеристики макроциклов в водной среде (ККА, размеры агрегатов, дзета-потенциал). Продемонстрировано, что образующиеся агрегаты обладают способностью солюбилизировать липофильный азокраситель Оранж ОТ, причем солюбилизирующая способность существенно возрастает при переходе от бутил- к тетрадецилпроизводным. С помощью методов динамического и электрофоретического рассеяния света и флуориметрии с бромистым этидием в качестве зонда показано, что полученные макроциклы взаимодействуют с ДНК тимуса теленка. Установлено, что на эффективность взаимодействия большое влияние оказывает длина оксиэтильных фрагментов: макроциклы, содержащие тетраэтилен-

гликолевые фрагменты более эффективны по сравнению с триэтиленгликолевыми аналогами, вызывая двукратную компактизацию ДНК.

Ключевые слова: Тиакаликс[4]арен, имидазол, амфифилы, ДНК тимуса теленка, этидий бромистый, солюбилизирующая емкость.

Introduction

Molecules with self-assembling properties are of great demand since they are used in creation of various functional colloid systems including those for practical applications.[1–3] Thus, amphiphilic molecules play a critical role in many fields, from household chemicals, food, cosmetics, pharmaceuticals to petrochemistry, catalysis, as well as biology and medicine.[4,5] Behavior of amphiphilic molecules in solutions is strongly dependent on their structure, that's why it is important to clearly understand the structure-aggregation relationship.[6] Imidazole-containing amphiphiles occupy a special place due to their unique properties: they can form supramolecular complexes with drugs, proteins, nucleic acids, and are also used as ionic liquids, basic components of nanogels and in organocatalysis.[7–10] The introduction of ethylene glycol fragments into amphiphilic molecules leads to an increase in their water solubility and improves biocompatibility.[11]

The calixarene platform allows to combine various functional groups on one platform. Moreover, easy synthesis and functionalization of calixarenes, as well as their low toxicity, make them promising molecular platforms for creating non-viral vectors for gene delivery as well as drug delivery agents.[12,13] Earlier we have proposed a convenient strategy for the synthesis of cationic amphiphiles based on the reaction of *p-tert*-butylthiacalix[4] arene in the *1,3-alternate* stereoisomeric form, containing long-chain alkyl fragments on one side of the macrocycle and bromoalkyl fragments on the other, with various tertiary amines and *N*-heterocycles.[14] Herein we present the synthesis of *tert*-butylthiacalix[4]arene amphiphiles in the *1,3-alternate* stereoisomeric form, containing oligoethyleneglycol fragments in addition to imidazolium ones in the polar region of the molecule, which increases the water solubility and bioaffinity of macrocycles. Their aggregation properties as well as interaction with the calf thymus DNA (TT DNA) are also discussed.

Experimental

Solvents were purified by standard methods.[15] All reagents were purchased from either Acros or Sigma-Aldrich and were used without further purification. 5,11,17,23-Tetra-*tert*-butyl-25,27-dibutyloxy-26,28-bis[4-bromobutyloxy]-2,8,14,20-tetrathiacalix[4]arene (**1**), 5,11,17,23-tetra-*tert*-butyl-25,27-ditetradecyloxy-26,28-bis[4-bromobutyloxy]-2,8,14,20-tetrathiacalix[4]arene (**2**), 1-(2-(2-(2-methyloxyethyloxy)ethyloxy)ethyl)-1*H*-imidazole (**3**), 1-(2-(2-(2-(2-methyloxyethyloxy)ethyloxy)ethoxy)ethyl)-1*H*-imidazole (**4**) were synthesized according to published methods.[16,17] The purity of the substances was controlled by thin layer chromatography using Merck Silica gel 60 F254 plates (HX68558954) with Vilber Lourmat VL-6.LC UV lamp (254 nm) control. NMR spectra were recorded on Bruker Avance 400 Nanobay with signals from residual protons of deuterated solvents ($CDCl_3$ or DMSO-d_6) as internal standard. The IR spectra of the synthesized compounds were recorded on a Bruker Vector-22 Fourier spectrometer in the wavenumber range of 400–4000 cm^{-1}; samples were prepared as thin films, obtained from chloroform solutions dried on the surface of the KBr tablet. ESI HRMS mass spectra were obtained on an Agilent 6550 iFunnel Q-TOF LC/MS spectrometer in positive mode. Elemental analysis was performed on a EuroVector EA 3000 CHN analyzer. The melting points of the substances were determined on a Stuart SMP10 compact heating table.

DLS and EDS experiments were performed on a Zetasizer Nano instrument (Malvern Instruments, USA) using a 10 mW 633 nm He – Ne laser; the data obtained were processed with the DTS program (Dispersion Technology Software 5.00). Experiments were performed in DTS 0012 plastic cuvettes (Sigma-Aldrich, USA) at 25 °C. For each sample, at least three measurements were carried out. Fluorescence experiments were performed in 10 mm quartz cuvettes on a Fluorolog FL-221 instrument (HORIBA Jobin Yvon). To measure the fluorescence of pyrene (0.001 mM), the following parameters were used: λ_{ex} = 335 nm, shooting range 350–430 nm; for the EB system (0.002 mM) – TT DNA (0.035 mM) – thiacalixarene in TRIS (25 mM, p*H* = 7.3): λ_{ex} = 480 nm, shooting range 530–700 nm.

The electronic absorption spectra of Orange OT were recorded in 10 mm quartz cuvettes on a Shimadzu UV-2700 spectrophotometer in the range of 350–700 nm. For this, solutions of thiacalixarenes of a certain concentration (0–2.25 mM) were added to the crystal dye Orange OT (3 mM), and the system was thermostated for 48 hours at room temperature.

General procedure for synthesis of compounds EGm-TCA-Cn (m = 3, 4, n = 4, 14): 0.18 mmol of dialkyl-dubromobutoxy *p-tert*-butylthiacalix[4]arene (**1** or **2**) and 1.8 mmol of ethoxyimidazole (**3** or **4**) were dissolved together in 3 mL of dry acetonitrile in 'GlassChem' vessel (CEM® corporation). The reaction mixture was stirred at 130 °C for 30–50 h. The reaction was controlled by TLC (petroleum ether: ethyl acetate = 1:4; R_f = 0 for the obtained imidazolium salts). After complete of reaction solvent was evaporated in *vacuo*, and formed precipitate was filtered off, washed with diethyl ether (2×20 mL). Obtained cream color powder was then dried in a vacuum desiccator for 12 h.

5,11,17,23-Tetra-tert-butyl-25,27-dibutyloxy-26,28-bis[4-(3-N-(2-(2-(2-methylethyloxy)ethyloxy)ethyl))imidazolium)butyloxy]-2,8,14,20-tetrathiacalix[4]arene dibromide **5** (EG3-TCA-C4). Weight: 0.24 g (83 %). HRMS (ESI) *m/z*: $[M\text{-}2Br\text{-}]^{2+}$ calcd. for $[C_{76}H_{114}N_4O_{10}S_4]^{2+}$ 685.3703, found: 685.3703. m.p. = 180 °C. IR (KBr) ν_{max} cm^{-1}: 2954 (-C-H_{Ar}), 1709 (-C=N-), 1266 (=C-O-). ^{1}H NMR ($CDCl_3$, 363 K) δ_H ppm: 0.79 (6H, t, CH_3, *J* = 7.2 Hz), 0.90–1.01 (4H, m, CH_2), 1.05–1.17 (8H, m, CH_2), 1.28 (36H, br.s, CMe_3, CMe_3), 1.79–1.87 (4H, m, CH_2), 3.38 (6H, s, OCH_3), 3.55 (4H, br.t, OCH_2), 3.59–3.65 (8H, m, OCH_2), 3.66 (4H, br.t, OCH_2), 3.79 (4H, t, OCH_2, *J* = 7.7 Hz), 3.84 (4H, t, OCH_2, *J* = 7.3 Hz), 3.90 (4H, br.t, NCH_2), 4.17 (4H, t, NCH_2, *J* = 7.6 Hz), 4.60 (4H, br.t, NCH_2), 7.28 (4H, s, ArH). 7.34 (4H, s, ArH), 7.52 (2H, br.d, ImH), 7.62 (2H, br.d, ImH), 10.55 (2H, s, ImH). ^{13}C NMR ($CDCl_3$) δ_C ppm: 14.02, 18.96, 25.74, 26.52, 30.61, 31.36, 31.50, 31.80, 34.35, 34.46, 49.56, 49.74, 59.13, 67.45, 68.72, 69.22, 70.39, 70.45, 71.95,

121.76, 123.53, 126.69, 127.78, 128.13, 128.66, 137.32, 145.83, 146.03, 156.63, 156.88.

5,11,17,23-Tetra-tert-butyl-25,27-ditetradecyloxy-26,28-bis[4-(3-N-(2-(2-(2-methylethyloxy)ethyloxy)ethyl))imidazolium) butyloxy]-2,8,14,20-tetrathiacalix[4]arene dibromide **6** (EG3-TCA-C14). Weight: 0.25 g (81 %). HRMS (ESI) *m/z*: $[M\text{-}2Br\text{-}]^{2+}$ calcd. for $[C_{96}H_{154}N_4O_{10}S_4]^{2+}$ 826.0285, found: 826.0285. m.p. = 77 °C. IR (KBr) ν_{max} cm^{-1}: 2925 (-C-H_{Ar}), 1734 (-C=N-), 1267 (=C-O-). ^1H NMR ($CDCl_3$, 363 K) δ_H ppm: 0.82–0.97 (6H, br.t, CH_3), 1.01–1.17 (12H, m, CH_2), 1.18–1.36 (72H, m, CH_2, CMe_3, CMe_3), 1.76–1.93 (4H, m, CH_2), 3.38 (6H, s, OCH_3), 3.55 (4H, br.t, OCH_2), 3.59–3.65 (12H, m, OCH_2), 3.66 (4H, br.t, OCH_2), 3.75 (4H, br.t, OCH_2), 3.84 (4H, br.t, OCH_2), 3.89 (4H, br.t, NCH_2), 4.17 (4H, br.t, NCH_2), 4.60 (4H, br.t, NCH_2), 7.26 (4H, s, ArH). 7.34 (4H, s, ArH), 7.52 (2H, br.d, ImH), 7.63 (2H, br.d, ImH), 10.52 (2H, s, ImH). ^{13}C NMR ($CDCl_3$) δ_C ppm: 14.24, 15.38, 22.81, 25.81, 25.89, 26.53, 28.76, 29.50, 29.77, 29.82, 30.11, 31.41, 31.52, 31.71, 32.05, 34.35, 34.44, 49.06, 49.52, 49.79, 59.12, 65.96, 67.42, 68.78, 69.26, 69.74, 70.23, 70.36, 70.41, 70.44, 70.53, 71.98, 120.99, 121.09, 121.76, 123.63, 126.57, 127.77, 127.94, 128.53, 137.11, 137.75, 146.08, 156.64, 156.73.

5,11,17,23-Tetra-tert-butyl-25,27-dibutyloxy-26,28-bis[4-(3-N-2-(2-(2-(2-methylethyloxy)ethyloxy)ethyloxy)ethyl))imidazolium) butyloxy]-2,8,14,20-tetrathiacalix[4]arene dibromide **7** (EG4-TCA-C4). Weight: 0.24 g (71 %). HRMS (ESI) *m/z*: $[M\text{-}2Br\text{-}]^{2+}$ calcd. for $[C_{80}H_{122}N_4O_{12}S_4]^{2+}$ 729.3966, found: 729.3969. m.p. = 177 °C. IR (KBr) ν_{max} cm^{-1}: 2921 (-C-H_{Ar}), 1734 (-C=N-), 1268 (=C-O-). ^1H NMR ($CDCl_3$, 363 K) δ_H ppm: 0.79 (6H, t, CH_3, J = 7.3 Hz), 0.88–1.01 (4H, m, CH_2), 1.01–1.18 (8H, m, CH_2), 1.28 (36H, br.s, CMe_3, CMe_3), 1.75–1.89 (4H, m, CH_2), 3.36 (6H, s, OCH_3), 3.54 (4H, br.t, OCH_2), 3.60–3.68 (20H, m, OCH_2), 3.76–3.93 (12H, m, OCH_2), 4.16 (4H, t, NCH_2, J = 7.8 Hz), 4.58 (4H, br.t, NCH_2), 7.27 (4H, s, ArH). 7.34 (4H, s, ArH), 7.56 (2H, br.d, ImH), 7.62 (2H, br.d, ImH), 10.48 (2H, s, ImH). ^{13}C NMR ($CDCl_3$) δ_C ppm: 13.96, 18.88, 25.67, 26.36, 30.53, 31.28, 31.72, 34.27, 34.38, 49.45, 49.62, 59.02, 67.34, 68.61, 69.18, 70.25, 70.30, 70.41, 70.45, 70.56, 71.89, 121.65, 123.48, 126.60, 127.69, 128.01, 128.55, 137.31, 145.77, 145.95, 156.52, 156.78.

5,11,17,23-Tetra-tert-butyl-25,27-ditetradecyloxy-26,28-bis[4-(3-N-2-(2-(2-(2-methylethyloxy)ethyloxy)ethyloxy)ethyl))imidazolium) butyloxy]-2,8,14,20-tetrathiacalix[4]arene dibromide **8** (EG4-TCA-C14). Weight: 0.29 g (84 %). HRMS (ESI) *m/z*: $[M\text{-}2Br\text{-}]^{2+}$ calcd. for $[C_{100}H_{162}N_4O_{12}S_4]^{2+}$ 870.0547, found: 870.0547. m.p. = 75 °C. IR (KBr) ν_{max} cm^{-1}: 2925 (C-H_{Ar}), 1726 (-C=N), 1267 (=C–O-). ^1H NMR ($CDCl_3$, 363 K) δ_H ppm: 0.83–0.91 (6H, br.t, CH_3), 1.02–1.18 (12H, m, CH_2), 1.18–1.23 (16H, m, CH_2), 1.23–1.37 (60H, m, CMe_3, CH_2), 1.75–1.90 (4H, m, CH_2), 3.36 (6H, s, OCH_3), 3.55 (4H, br.t, OCH_2), 3.58–3.69 (20H, m, OCH_2), 3.76 (4H, t, OCH_2, J = 7.7 Hz), 3.84 (4H, t, OCH_2, J = 7.0 Hz), 3.89 (4H, br.t, OCH_2), 4.16 (4H, t, NCH_2, J = 7.6 Hz), 4.59 (4H, br.t, NCH_2), 7.26 (4H, br.s, ArH). 7.34 (4H, s, ArH), 7.58 (2H, br.d, ImH), 7.64 (2H, br.d, ImH), 10.50 (2H, c, ImH). ^{13}C NMR ($CDCl_3$) δ_C ppm : 14.25, 22.81, 25.80, 25.87, 26.48, 28.76, 29.50, 29.77, 29.80, 30.11, 31.40, 31.51, 31.61, 31.78, 32.04, 34.34, 34.45, 47.57, 49.55, 49.75, 59.09, 67.48, 68.85, 69.20, 70.34, 70.38, 70.48, 70.62, 71.97, 121.74, 121.74, 123.64, 123.64, 126.59, 126.59, 127.73, 127.73, 128.18, 128.18, 128.65, 128.65, 137.30, 137.30, 145.85, 145.85, 146.10, 146.10, 156.68, 156.68, 156.77.

Results and Discussion

Synthesis of ethyleneglycol macrocycles

Bromine derivatives of thiacalixarene **1**–**2** were chosen as precursors for the synthesis of imidazolium oxyethyl salts. They were synthesized using literature method[14] by the stepwise selective functionalization of the lower rim of the initial *p-tert*-butyl-thiacalix[4]arene under the Mitsunobu reaction conditions followed by the introduction of bromobutyl groups using Williamson reaction. The quaternization of the starting imidazoles **3**–**4** with thiacalix[4]arenes **1**, **2** was carried out in acetonitrile in a 'GlassChem'

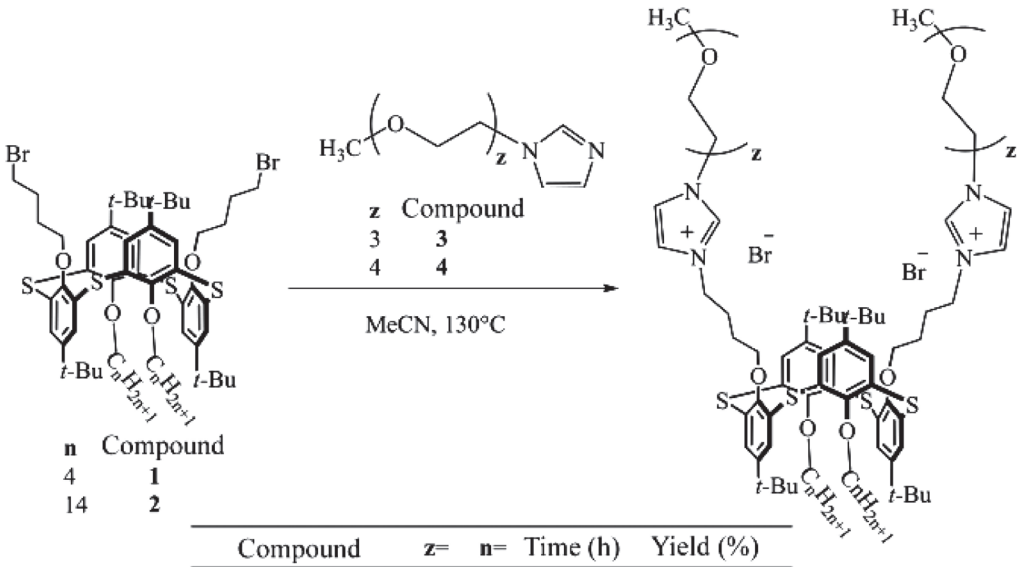

Compound	z=	n=	Time (h)	Yield (%)
5 (EG3-TCA-C4)	3	4	50	83
6 (EG3-TCA-C14)	3	14	30	81
7 (EG4-TCA-C4)	4	4	50	78
8 (EG4-TCA-C14)	4	14	30	84

Scheme 1. Synthesis of imidazolium ethylene glycol salts based on *p-tert*-butylthiacalix[4]arene.

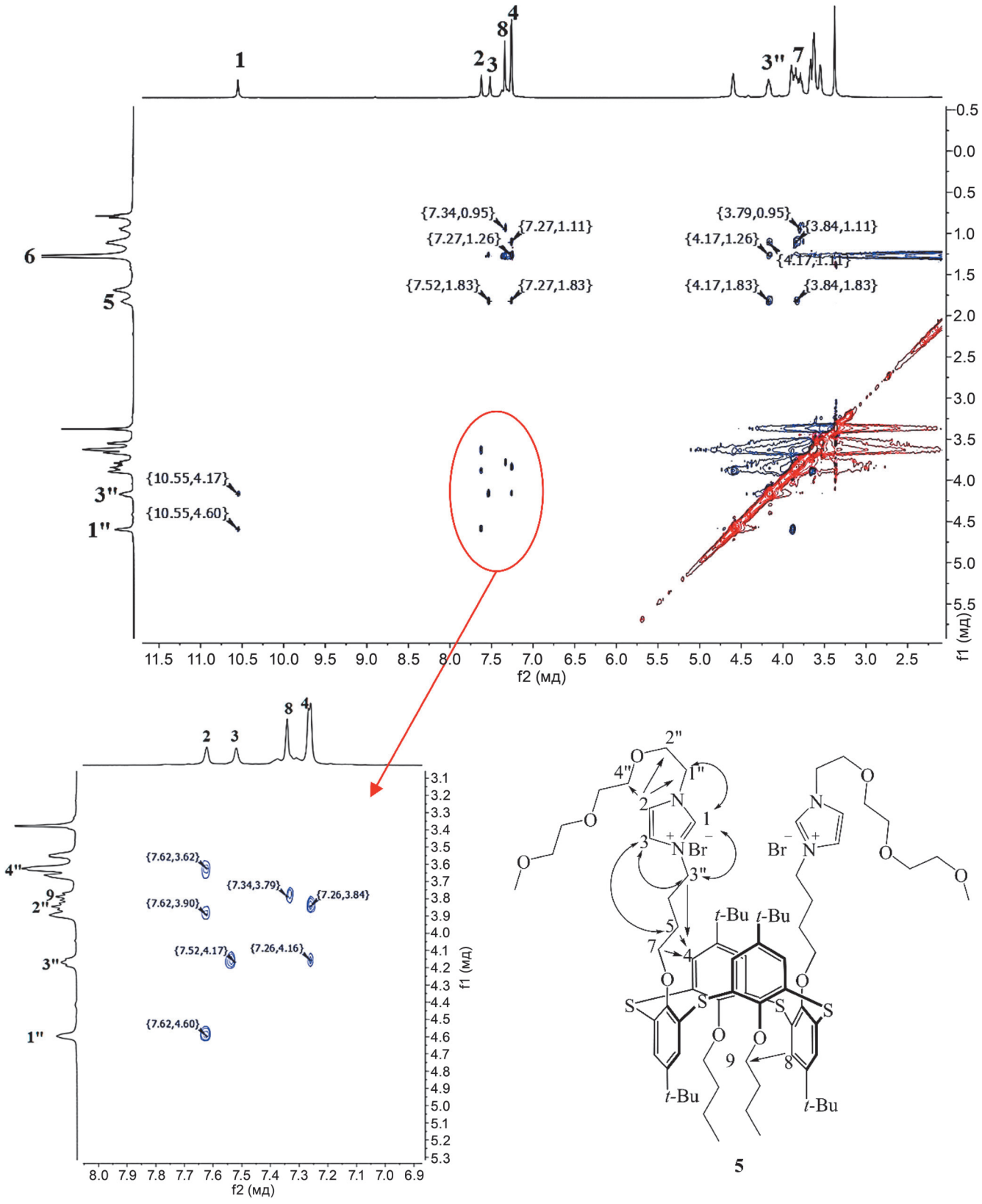

Figure 1. Fragments of NMR (^{1}H-^{1}H) NOESY spectrum of **5** (DMSO-d_6).

glass autoclave (CEM® corporation) at 130 °C (Scheme 1). It was found that conversion of reaction is strongly dependent on the solubility of initial macrocycles in acetonitrile. Thus, due to the good solubility of the macrocycle **2** with tetradecyl alkyl fragments in acetonitrile, the reaction was finished after 30 hours, while for di-butyl derivative **1** it took 50 hours. Macrocycles with tetradecyl alkyl fragments were proved to be classical ionic liquids, melting within the range of 75–78 °C, which is obviously associated with the bad packing of long-chain alkyl and oxyethyl fragments.

The structure of the synthesized compounds was proved by a set of physical research methods: NMR, IR spectroscopy,

ESI-HRMS spectrometry, and the composition – by elemental analysis. Signal assignment in the ^{1}H NMR spectra was carried out using 2D NMR – NOESY experiments. As an example, Figure 1 shows the (^{1}H-^{1}H) NOESY spectrum of compound **5**. The spectrum exhibits cross-peaks between the signals of methylene protons of the ethylene glycol fragment 1" (δ = 4.60 ppm) and imidazole protons 1 (δ = 10.55 ppm). between the signals of methylene protons of the butylene linker 3" (δ = 4.17 ppm) and imidazole protons 1 (δ = 10.55 ppm), between the signals of imidazole protons 3 (δ = 7.52 ppm) and signals of methylene protons of the linker 3" (δ = 4.17 ppm), between the signals of imidazole protons 2 (δ = 7.62 ppm) and methylene protons of the ethylene glycol fragment 1", 2", 4" (δ = 4.60, 3.90, 3.62 ppm), between the signals of methylene protons of the butylene linker 3" (δ = 4.17 ppm) and aromatic protons 4 (δ = 7.26 ppm), and between the signals of aromatic protons 8 (δ = 7.34 ppm) and oxymethylene protons of butyl substituents 9 (δ = 3.79 ppm), which clarifies that the compound EG3-TCA-C4 is in the 1,3-*alternate* stereoisomeric form.

Compounds composition was confirmed by high resolution ESI mass spectrometry (ESI-HRMS). According to the obtained data, in all compounds the molecular ion $[M\text{-}2Br]^{2+}$ is formed by repulsion of two bromine atoms (Figure 2).

Study of EGm-TCA-Cn aggregation in aqueous solutions

The obtained thiacalixarenes **5**–**8** were proved to be readily soluble in water and aqueous-buffered TRIS solution, forming supramolecular associates with critical aggregation concentrations (CACs) presented in Table 1.

The CAC values were established using a fluorescent probe – pyrene, for which the intensity ratios of the first (373 nm) and third (383 nm) maxima in the emission spectrum are extremely sensitive to a change in the polarity of the medium (Figure 3A).[18,19]

According to dynamic (DLS) and electrophoretic light scattering (ELS) data (Table 1), EGm-TCA-Cn form submi-

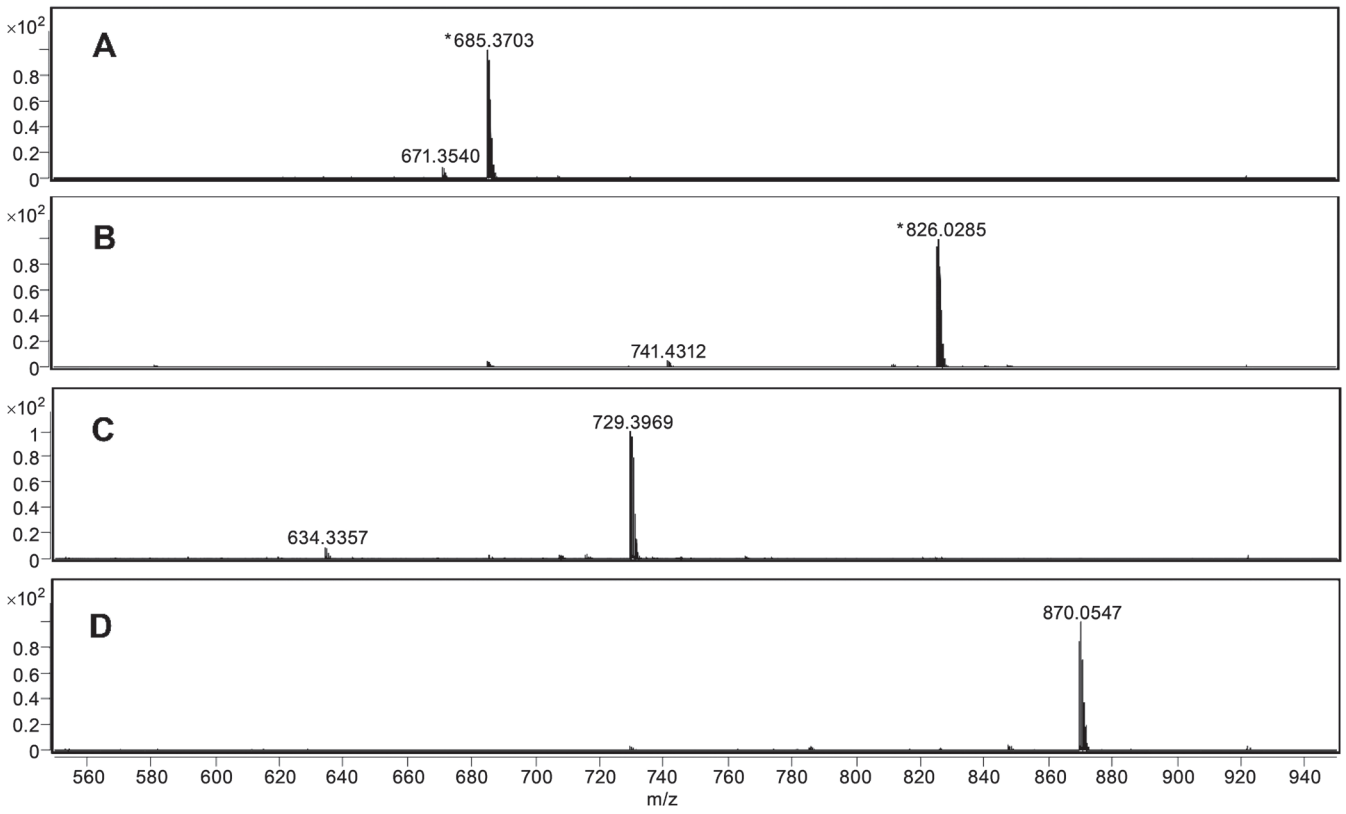

Figure 2. ESI-HRMS spectra of EG3-TCA-C4 (A), EG3-TCA-C14 (B), EG4-TCA-C4 (C), EG4-TCA-C14 (D).

Table 1. CAC, DLS and ELS data of the aqueous solutions of EG*m*-TCA-C*n* (*m* = 3, 4, *n* = 4, 14).

TCA	CAC, mM	Concentration of TCA, мМ	PDI	Average hydrodynamic size, nm	Zeta-potential, mV
EG3-TCA-C4	0.890	1.335	0.747 ± 0.029	925 ± 34	+59 ± 1
EG3-TCA-C14	0.048	0.072	0.567 ± 0.031	523 ± 5	+43 ± 1
EG4-TCA-C4	1.65	2.475	0.470 ± 0.190	470 ± 20	+55 ± 3
EG4-TCA-C14	0.017	0.026	0.465 ± 0.045	345 ± 5	+66 ± 2

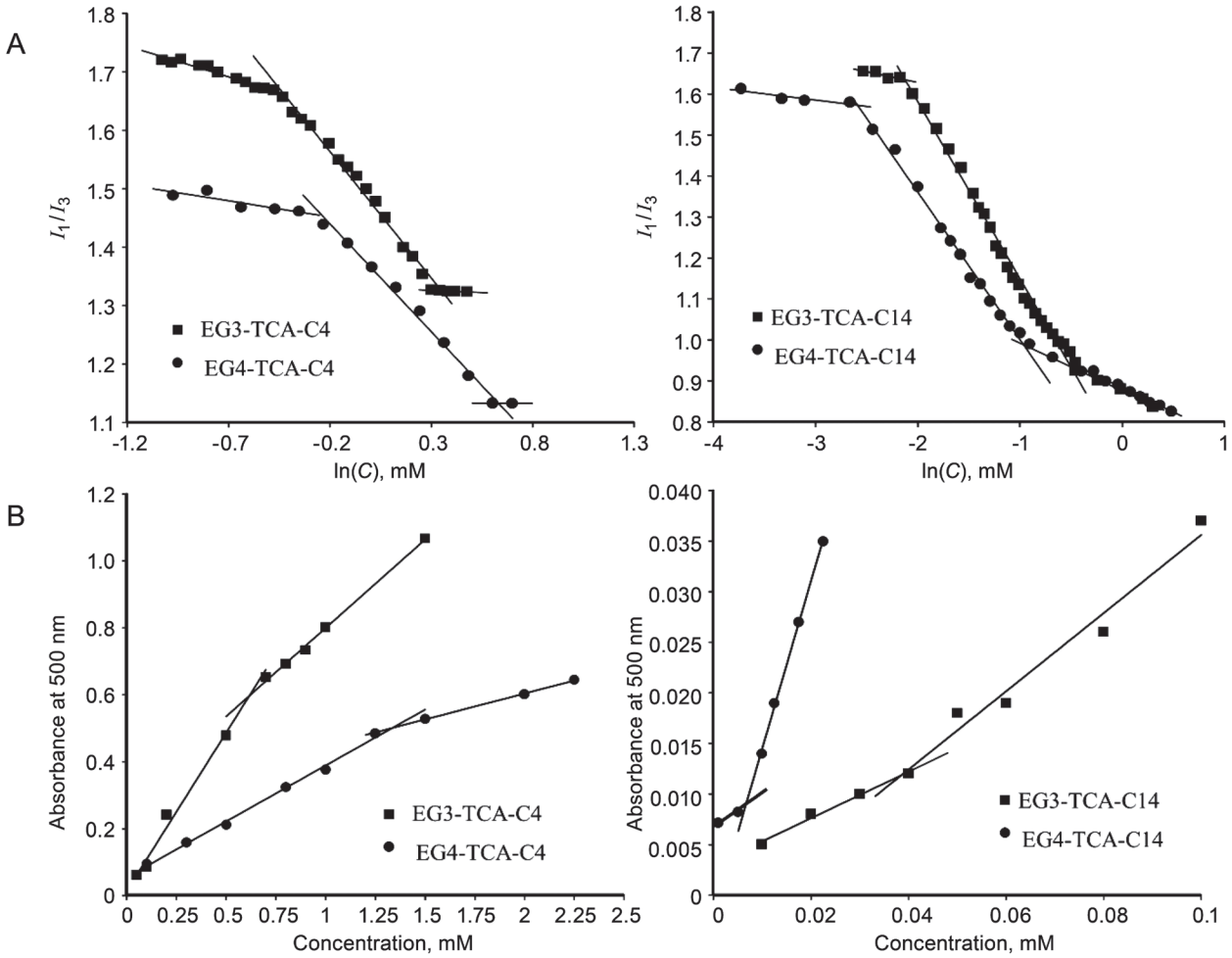

Figure 3. (A) Dependence of I(373nm)/I(384 nm) pyrene ratio *vs.* lg(*C*) of EG*m*-TCA-C*n* (*m* = 3, 4, *n* = 4, 14) in system: G*m*-TCA-C*n* / pyrene; (B) dependence of absorbance at 500 nm of Orange OT *vs*. concentration of EG*m*-TCA-C*n* in system: G*m*-TCA-C*n* / Orange OT; *C*(pyrene) = 0.001 mM, *C*(Orange OT)=3 mM, 25 °C.

cron particles with high positive zeta potentials. According to the data obtained, tetraethylene glycol calixarenes EG4-TCA-C4 and EG4-TCA-C14 form more compact aggregates compared to triethylene glycol derivatives EG3-TCA-C4 and EG3-TCA-C14. Also, when passing to tetraethylene glycol derivatives, the polydispersity index decreases. This behavior can be associated with a change in the critical packing parameter, which is the ratio of the volume of the hydrophobic and hydrophilic parts of the amphiphile:[20] a change in the geometry of the molecule due to an increase in the volume of the polar part of the molecule can lead to a change in the shape of the aggregates. Considering that the critical packing parameter of calix[4]arenes in the *1,3-alternate* configuration is usually ≈ 1, the formation of bilayer structures including vesicles is most expected for them.[21,22]

The presence of a hydrophobic zone in EG*m*-TCA-C*n* associates (*m* = 3, 4, *n* = 4, 14) suggests the possibility of binding of water-insoluble substrates. The water-insoluble dye Orange OT was chosen as a model substrate. Dye solubilization was controlled using the changes in the optical density of the dye at 500 nm in the UV-visible spectrum (Figure 3B). The results showed that Orange OT is soluble in water only in the presence of EG*m*-TCA-C*n* (*m* = 3, 4, *n* = 4, 14), and the solubility of the dye depends on the concentration of thiacalixarene, which also can be used to determine the CAC values.[23] As can be seen from Table 2, the CAC values obtained by spectrophotometric solubilization of Orange OT are close to the values obtained by the pyrene method. In the case of the more lipophilic tetradecyl-containing macrocycles EG3-TCA-C14 and EG4-TCA-C14, an insignificant increase in the absorption intensity at 500 nm is observed, which indicates that the dye is bound by individual macrocycles. When the CAC is reached, an increase in the absorption intensity is observed, which indicates the solubilization of the dye in the hydrophobic zone of the aggregates. However, in the case of less lipophilic butyl-containing macrocycles EG3-TCA-C4 and EG4-TCA-C4, another picture is observed. With an increase in the concentration of the macrocycle, a linear increase in the solubilization of the dye by individual macrocycles occurs, slowing down after the macrocycles reach CAC. This slowdown is associated with the extremely low solubilizing ability of the aggregates due to the insufficient hydrophobicity of the short butyl fragments. The solubilizing ability of the aggregates (*S*), which corresponds to the number of moles of the dye solubilized with one mole of the surfactant, is determined according

to the equation:[24] $S = B/(\varepsilon_{ext} \cdot l)$, where B is the slope parameter (the tangential angle of the dependence of the optical density of the dye on the content surface-active substance at a concentration higher than CAC), and ε_{ext} is the extinction coefficient of the dye (ε_{ext} = 17400 M^{-1} cm^{-1}).[25] From the results obtained (Table 2), it follows that the solubilizing ability of EG4-TCA-C14 is higher than that of the classical surfactant – CTAB (S = 15 mM[26]), as well as surfactants with bulky head groups DABCO-14 (S = 18.9 mM[27]), triphenylphosphonium bromides (S = 27.7 mM[28]), and for imidazole-containing surfactants (S = 20–50 mM[29]), which opens up the prerequisites for the use of the macrocycles as non-viral vectors or drug delivery vehicles.

Table 2. CAC and solubilization ability (total and of the aggregates) in relation to the hydrophobic dye Orange OT; 25 °C.

	CAC, mM	S_{tot}, OT(M) / EG*m*-TCA-C*n*, мМ	S_{agr}, mM
EG3-TCA-C4	0.712	30	50
EG3-TCA-C14	0.048	22	1830
EG4-TCA-C4	1.341	8.8	17
EG4-TCA-C14	0.038	95	11800

However, it should be kept in mind that the formula for determining the solubilizing ability S does not take into account the amount of dye absorbed by individual molecules of the macrocycle before reaching the CAC, which however can reach very significant values. Thus, before reaching CAC, the EG3-TCA-C4 macrocycle already has time to solubilize 0.04 mM of the dye, while the EG3-TCA-C14 macrocycle is 0.0007 mM. This is a result of the large difference in their CAC. For a more correct comparison of the solubilizing ability of aggregates, it is convenient to estimate the corrected solubilizing ability of aggregates (S_{agr}), which takes into account the amount of adsorbed dye before reaching the CAC and is determined by the formula $S_{agr} = S_{tot} / A_{CAC}$, where A_{CAC} is the absorption of the dye at the point where the CAC of the macrocycle is reached. In this case, it becomes obvious that the aggregates formed by more hydrophobic tetradecyl macrocycles are tens of times more efficient in solubilizing the dye.

Interaction of EGm-TCA-Cn with calf thymus DNA

To assess the possibility of using the obtained macrocycles as non-viral vectors for the delivery of gene material, their interaction with a model nucleic acid, TT DNA, was studied.[30,31] To study the interaction, we used the fluorescence method with ethidium bromide (EB) as a fluorescent label: the intrinsic fluorescence of EB is extremely low, but when it intercalates between DNA base pairs, the fluorescence intensity increases significantly. Intercalation of DNA by another molecule leads to competitive displacement of EB and, as a consequence, to quenching of fluorescence.[32] The degree of fluorescence quenching of EB-DNA can be used to determine the degree of binding between a competing molecule and DNA.[33] The maximum emission of EB under excitation λ_{exc} = 480 nm appears at 590 nm (Figure 4).

When ethylene glycol derivatives of thiacalixarene are added to the solution of the TT DNA – EB complex, substantial quenching of EB luminescence is observed. The observed hypochromism indicates the displacement of EB molecules from the corresponding centers of TT DNA. All studied macrocycles, except for EG3-TCA-C4, effectively displace EB, causing 9–13-fold quenching of fluorescence. The plots of fluorescence quenching in Stern-Volmer coordinates for all studied macrocycles are nonlinear, which indicates a mixed static and dynamic mechanisms of EB luminescence quenching[9,34] and makes the calculation of the quenching

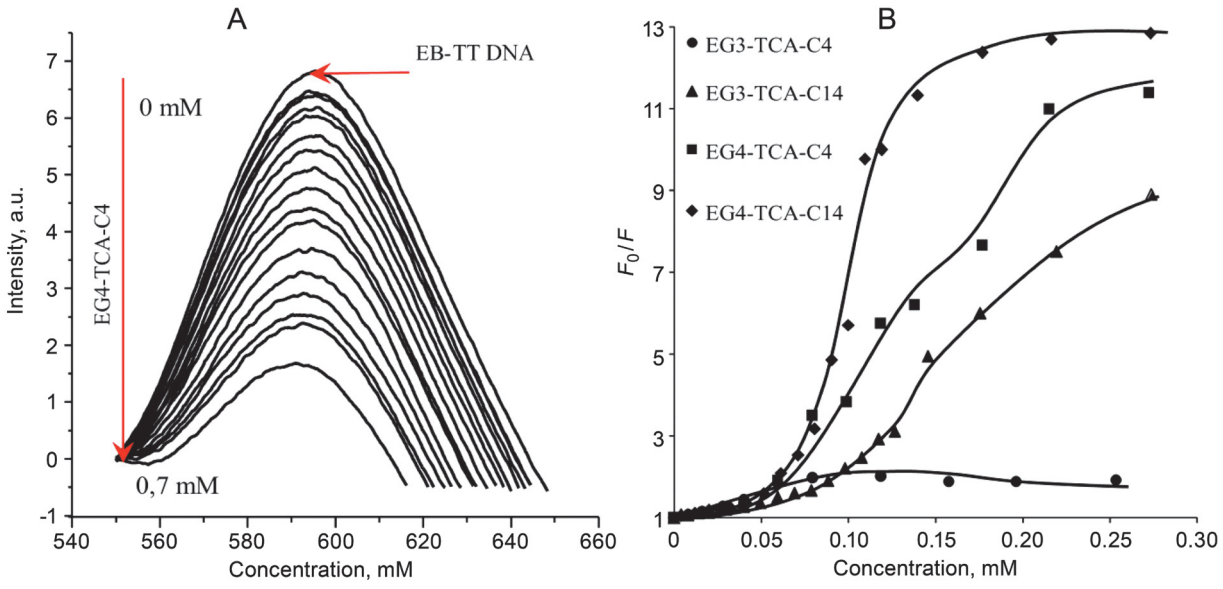

Figure 4. Fluorescence spectra of EB in the TT DNA – thiacalixarene EG4-TCA-C4 system (A) and Stern-Volmer plots of the macrocycles (B), where F_0/F is the ratio of the luminescence intensities of EB-TT DNA at 590 nm in the absence and presence of the studied macrocycles. C(EB) = 0.002 mM, C(TT DNA) = 0.025 mM, H_2O, 25 °C.

Table 3. Average hydrodynamic diameter and electrophoretic potential in aqueous solutions containing EG*m*-TCA-C*n* (0.15 mM) and TT DNA (0.025 mM).

	Average hydrodynamic size, nm	PDI	Zeta-potential, mV
TT DNA	900 ± 80	0.200 ± 0.030	–26 ± 1
TT DNA+EG3-TCA-C4	870 ± 8	0.605 ± 0.011	+68 ± 2
TT DNA+EG3-TCA -TCA-C14	795 ± 60	0.590 ± 0.025	+41 ± 2
TT DNA+EG4-TCA-C4	390 ± 1	0.500 ± 0.013	+53 ± 2
TT DNA+EG4-TCA-C14	400 ± 5	0.522 ± 0.056	+67 ± 1

constant incorrect. It is known that imidazolium amphiphilic molecules are capable of interacting with DNA both through hydrophobic interactions and through intercalation incorporation.[35] Based on the data obtained, it becomes obvious that the efficiency of the interaction of macrocycles with TT DNA depends on both the hydrophobicity and the length of the oxyethylated fragments. Moreover, the determining factor is the presence of tetraoxyethylated fragments – macrocycles EG4-TCA-C4 and EG4-TCA-C14 cause the greatest quenching of EB fluorescence, the EG3-TCA-C14 macrocycle is less effective, and EG3-TCA-C4 causes only insignificant quenching of EB fluorescence. A similar dependence of the efficiency of interaction of molecules with DNA on the length of oxyethylated fragments was previously shown in several works.[36,37] Presumably, longer oxyethylated fragments interact more efficiently with DNA base pairs via hydrogen bonding.

For a detailed study of the mechanism of TT DNA binding to EG*m*-TCA-C*n*, solutions containing TT DNA and EG*m*-TCA-C*n* at a concentration of 0.2 mM, corresponding to the maximum binding concentration and higher than CAC, were studied by DLS and ELS (Table 3). According to DLS data, the average hydrodynamic diameter of TT DNA is 900 ± 80 nm, while the polymer has a negative electrophoretic potential (≈ –26 mV). A low value of the polydispersity index (0.200) indicates a narrow distribution of large globules.

The addition of EG4-TCA-Cn macrocycles (n = 4, 14) results in almost two-fold compaction of DNA, which does not occur with the addition of EG3-TCA-Cn (n = 4, 14). The data obtained are in good consistent with the EB release, which was effectively released upon interacting with tetraethylene glycol macrocycles.

Conclusions

For the first time, amphiphilic derivatives of *p-tert*-butylthiacalix[4]arene with various *O*-alkyl substituents at the lower rim and tri- and tetraethylene glycol imidazolium fragments at the upper rim were obtained. It was found that these macrocycles form stable sub-micron aggregates with a surface potential of + 40–60 mV. It was found that among the compounds obtained, tetradecyl-containing calixarenes have the highest solubilizing capacity, binding the hydrophobic Orange Ot dye in aqueous solutions. Using the dynamic and electrophoretic light scattering methods as well as fluorimetry with EB as a probe, it was shown that the obtained macrocycles interact with the calf thymus DNA. It was found that macrocycles containing tetraethylene glycol fragments interact with DNA more efficiently in comparison with triethylene glycol ones, causing a 2-fold compaction of DNA. Thus, the obtained amphiphiles have potential for use in biotechnology both for the creation of hydrophobic substrates delivery vehicles and for the creation of non-viral vectors.

Acknowledgement. We thank the Russian Science Foundation for the financial support of this work (grant No. 18-73-10033).

References

1. Chowdhury S., Rakshit A., Acharjee A., Saha B. *ChemistrySelect* **2019**, *4*, 6978–6995.
2. Li H., Zhao J., Wang A., Li Q., Cui W. *Colloids Surf. A*. **2020**, *590*, 24486.
3. Muraoka T., Honda H., Nabeya K., Kinbara K. *Chem. Commun.* **2020**, *56*, 7881–7884.
4. Schramm L.L., Stasiuk E.N., Marangoni D.G. *Annu. Rep. Prog. Chem., Sect. C: Phys. Chem.* **2003**, *99*, 3–48.
5. Kulkarni C. *Cosmetics* **2016**, *3*(4), 37.
6. *Encyclopedia of Membranes* (Drioli E., Giorno L., Eds.), Springer, Berlin, Heidelberg **2014**. 60 p.
7. Seo S.H., Tew G.N., Chang J.Y. *Soft Matter* **2006**, *2*, 886–891.
8. Zhang B., Jiang Z., Zhou X., Lu S., Li J., Liu Y., Li C. *Angew. Chem.* **2012**, *124*, 13336–13339.
9. Ibragimova, R.R., Burilov V.A., Aimetdinov A.R., Mironova D.A., Evtugyn V.G., Osin Y.N., Solovieva S.E., Antipin I.S. *Macroheterocycles* **2016**, *9*, 433–441.
10. Burilov V., Garipova R., Sultanova E., Mironova D., Grigoryev I., Solovieva S., Antipin I. *Nanomaterials* **2020**, *10*, 1143.
11. Parshad B., Prasad S., Bhatia S., Mittal A., Pan Y., Mishra P.K., Sharma S.K., Fruk L. *RSC Adv.* **2020**, *10*, 42098–42115.
12. Kashapov R.R., Razuvayeva Y.S., Ziganshina A.Y., Mukhitova R.K., Sapunova A.S., Voloshina A.D., Zakharova L.Ya. *Macroheterocycles* **2019**, *12*, 346–349.
13. Kashapov R.R., Gaynanova G.A., Gabdrakhmanov D.R., Kuznetsov D.M., Pavlov R.V., Petrov K.A., Zakharova L.Y., Sinyashin O.G. *Int. J. Mol. Sci.* **2020**, *21*, 6961.
14. Burilov V.A., Ibragimova R.R., Gafiatullin B.H., Nugmanov R.I., Solovieva S.E., Antipin I.S. *Macroheterocycles* **2017**, *10*, 215–220.
15. Armarego W.L.F., Chai C.L.L. *Purification of Laboratory Chemicals, 6th ed.,* Butterworth-Heinemann, **2009**. 743 p.
16. Burilov V.A., Nugmanov R.I., Ibragimova R.R., Solovieva S.E., Antipin I.S. *Mendeleev Commun*. **2015**, *25*, 177–179.
17. Bara J.E. *Ind. Eng. Chem. Res.* **2011**, *50*, 13614–13619.
18. Yan M., Li B., Zhao X. *Food Chem*. **2010**, *122*, 1333–1337.

19. Aguiar J., Carpena P., Molina-Bolıvar J.A., Ruiz C.C. *Colloid Interface Sci.* **2003**, *258*, 116–122.
20. Israelachvili J.N., Mitchell D.J., Ninham B.W. *J. Chem. Soc. Faraday Trans.* **1976**, *72*, 1525–1568.
21. Arimori S., Nagasaki T., Shinkai S. *J. Chem. Soc. Perkin Trans. 2* **1995**, *887*, 679–683.
22. Burilov V.A., Mironova D.A., Ibragimova R.R., Solovieva S.E., Konig B., Antipin I.S. *RSC Adv.* **2015**, *5*, 101177–101185.
23. Tehrani-Bagha A.R., Holmberg K. *Materials* **2013**, *6*, 580–608.
24. Zhiltsova E.P., Pashirova T.N., Ibatullina M.R., Lukashenko S.S., Gubaidullin A.T., Islamov D.R., Kataeva O.N., Kutyreva M.P., Zakharova L.Y. *Phys. Chem. Chem. Phys.* **2018**, *20*, 12688–12699.
25. Kashapov R.R., Kharlamov S.V., Sultanova E.D., Mukhitova R.K., Kudryashova Y.R., Zakharova L.Y., Ziganshina A.Y., Konovalov A.I. *Chem. – Eur. J.* **2014**, *20*, 14018.
26. Zakharova L.Y., Kashapov R.R., Pashirova T.N., Mirgorodskaya A.B., Sinyashin O.G. *Mendeleev Commun.* **2016**, *26*, 457–468.
27. Zakharova L.Y., Gaysin N.K., Gnezdilov O.I., Bashirov F.I., Kashapov R.R., Zhiltsova E.P., Pashirova T.N., Lukashenko S.S. *J. Mol. Liq.* **2012**, *167*, 89–93.
28. Gainanova G.A., Vagapova G.I., Syakaev V.V., Ibragimova A.R., Valeeva F.G., Tudriy E.V., Galkina I.V., Kataeva O.N., Zakharova L.Ya., Latypov S.K., Konovalov A.I. *J. Colloid Interface Sci.* **2012**, *367*, 327–336.
29. Kuznetsova D.A., Gabdrakhmanov D.R., Kuznetsov D.M., Lukashenko S.S., Sapunova A.S., Voloshina A.D., Nizameev I.R., Kadirov M.K., Zakharova L.Y. *J. Mol. Liq.* **2020**, *319*, 114094.
30. Ostos F.J., Lebron J.A., Moyá M.L., Deasy M., López-Cornejo P. *Colloids Surf.* **2015**, *127*, 65–72.
31. Rodik R.V., Anthony A.S., Kalchenko V.I., Mély Y., Klymchenko A.S. *New J. Chem*. **2015**, 39, 1654–1664. f
32. Zhou C.Y., Zhao J., Wu Y.B., Yin C.X., Pin Y. *J. Inorg. Biochem.* **2006**, *101*, 10–18.
33. Guo Q., Lu M., Marky L.A., Kallenbach N.R. *Biochemistry* **1992**, *31*, 2451–2455.
34. Izumrudov V.A., Zhiryakova M.V., Goulko A.A. *Langmuir* **2002**, *18*, 10348–10356.
35. Samarkina D.A., Gabdrakhmanov D.R., Lukashenko S.S., Khamatgalimov A.R., Kovalenko V.I., Zakharova L.Y. *Colloids Surf. A* **2017**, *529*, 990–997.
36. Shi P., Jianga Q., Zhang Q., Tian Y. *J. Organomet. Chem.* **2016**, *804*, 66–72.
37. Kumara V., Naik V.G., Das A., Bal S.B., Biswas M., Kumar N., Ganguly A., Chatterjee A., Banerjee M. *Tetrahedron* **2019**, *75*, 3722–3732.

Received 26.03.2021
Accepted 10.05.2021